Proceedings World Geothermal Congress 2020+1
Reykjavik, Iceland, April - October 2021

Geothermal Exploration of the Mesillas Zone, Nayarit, Mexico

Mariana P. Jácome-Paz, Irving A. González-Romo, Daniel Pérez-Zárate, Rosa M. Prol-Ledesma, Aurora M. Estrada-Murillo, Héctor Aviña-Jiménez and Daniel González.

Instituto de Geofísica. Circuito Exterior s/n Ciudad Universitaria. UNAM. Col Universidad. Coyoacán. 04510

jacome@igeofisica.unam.mx

Keywords: geothermal energy, thermal springs, diffuse emission, hydrogeochemistry

ABSTRACT

As part of the project between the IDEEA group of the Institute of Engineering and the Geothermal Research Group of the Geophysics Institute, UNAM, first exploration fieldwork has been carried out in the Mesillas geothermal system, Nayarit, Mexico with the long-term objective of developing a direct use geothermal project. A geological survey, chemical characterization of geothermal samples, diffuse flux analysis (CO_2, H_2S and CH_4) as well as reservoir temperature estimations in the geothermal system were performed. The Mesillas geothermal area (~ 420 m.a.s.l.) is in the southern part of the state of Nayarit, approximately 30 km west of San Pedro Lagunillas, where the geothermal field San Pedro Dome is located, which is currently under exploitation.

In general, the following preliminary results were obtained: (i) five andesitic units were identified in an area of ~1.5 km^2, with 25 thermal springs with discharge temperatures between 47-90 °C, pH ~ 9 and Na-CO_3 water type; (ii) andesites show high permeability given the intense fracturing derived from the normal faulting systems with trend NW-SE, SW-NE, NS, and EW; (iii) the surface hydrothermal alteration is argillic and (iv) degassing of CO_2 is restricted to the springs area with no preferential degassing direction.

1. INTRODUCTION

The interest in the use of geothermal resources in Mexico promotes exploration of new geothermal zones as part of the national strategy for the development of clean energy resources. The last six years, the Ministry of Energy allocated funds for the exploration of new areas of geothermal interest (Romo-Jones et al. 2017). Despite the governmental interest in the development of geothermal exploitation in new areas, during last decade few works have been published in Mexico with preliminary geothermal exploration (e.g. Iglesias et al. 2005; Arango-Galván et al. 2015). Specifically, in some of the reported locations, only geochemical exploration was carried out, (records of physicochemical parameters and chemical composition of thermal fluids). The main objective of geochemical exploration is to carry out reconnaissance work that includes i) the chemical-isotopic characterization of hydrothermal fluids discharged in geothermal areas, ii) the quantification of the diffuse dynamic degassing of soils and the bubbling springs, and iii) the estimation of the temperatures at depth using chemical geothermometers, which will be of great value to plan more detailed exploration programs in the future. This exploration allows to estimate temperatures at depth of the hydrothermal reservoir and, in many occasions, to generate a conceptual model of the processes during the ascent of fluids. In addition, it is the basis for geophysical exploration planning and a better delimitation of the reservoir.

In this work we describe the results of the geochemical and geological exploration in Mesillas, Nayarit, Mexico. There is no available information about previous geothermal exploration in the area; however, the Molote (the name of the closest town to Mesillas thermal area) hot springs are reported in the table of the Geothermal Anomalies Registry of the TransMexican Volcanic Belt, (González Ruiz et al. 2015). Mesillas area is a new exploration zone with a promising future to develop direct uses of geothermal energy**.**

1.1 Geological Settings

Mesillas area is located southwest of the state of Nayarit, approximately 33 km from Tepic, in the western part of the Trans-Mexican Volcanic Belt, sub-province of Sierra Neovolcanica Nayarita, which is bounded to the north by the Sierra Madre Occidental (SMO) and to the south by the Sierra Madre del Sur (SMS) (Figure 1).

Mesillas area is in the northwest part of the Jalisco Block that has a triple continental junction with the North American plate and the Michoacán block, with the triple system arms being the Rifts of Colima, Chapala and Tepic-Zacoalco (Figure 2). It has a different preferential direction of movement with respect to the tectonic plates of Rivera and North America and is considered a microplate (Stock et al, 1993). The Jalisco block is limited to the southeast by the rift of Colima which contains several volcanoes such as the Fuego volcano; to the east is the Chapala rift with an orientation NEE. Urrutia-Fucugauchi and Rosas-Elguera (1994) based on paleomagnetic studies, described its origin during the Miocene from a left lateral fault within the zone of the regional fault Chapala-Tula with trend EW. Towards the northeast, it is delimited by the Tepic-Zacoalco rift, a NW-oriented structure composed of a series of grabens and semigrabens developed during late Miocene (Ferrari and Rosas Elguera, 2000).

The volcanic activity of the western portion of the FVTM had great activity during late Miocene consisting mainly of basaltic plateaus, extending from Nayarit to Veracruz and showing a temporary distribution with the youngest volcanic structures to the east of the FVTM (Gómez-Tuena et al., 2005; Ferrari et al., 2000b; Ferrari, 2004; Ferrari et al., 2005b).

During late Pliocene-Quaternary (<3 Ma), volcanism has had a compositional change to andesitic-basaltic intraplate type, which generated the main stratovolcanoes west of the FVTM such as Tequila, Ceboruco, San Juan and Sangangüey (Figure 2). These volcanoes are distributed following regional WNW-ESE orientation faults that delimit the Jalisco block (Righter et al., 1995; Schaaf et al., 1995; Gómez-Tuena et al., 2005). The closest Volcano is located north of the study area, called El Molote Volcano, but there is no available information on its age or last eruptive event.

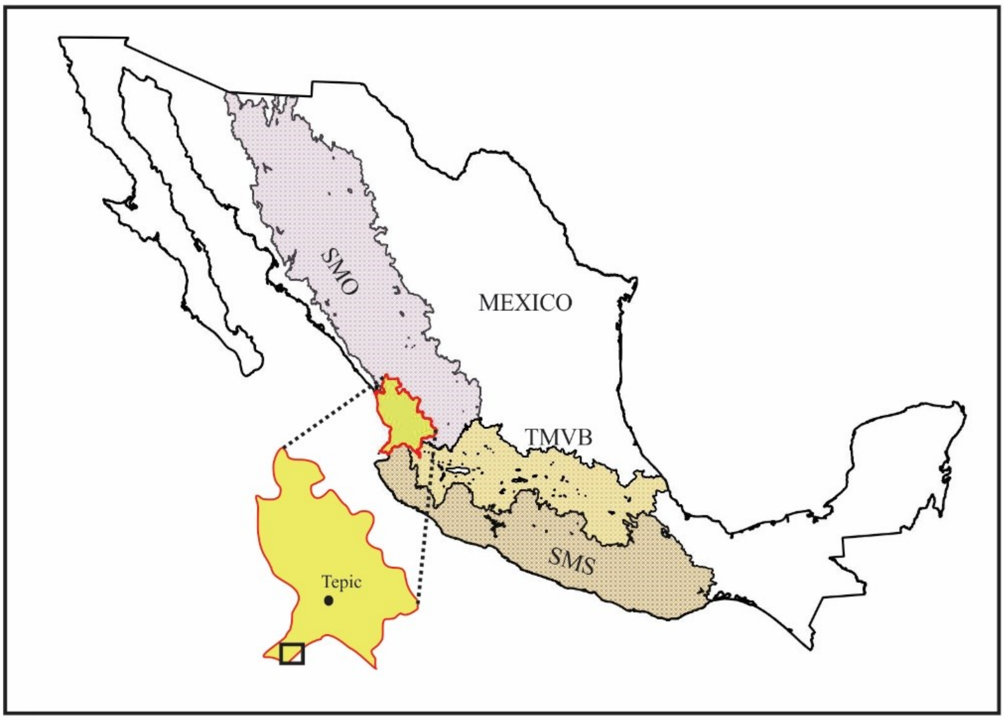

Figure 1: Location of Mesillas, Nayarit. Sierra Madre Occidental (SMO), Transmexican Volcanic Belt (FVTM), Sierra Madre del Sur (SMS).

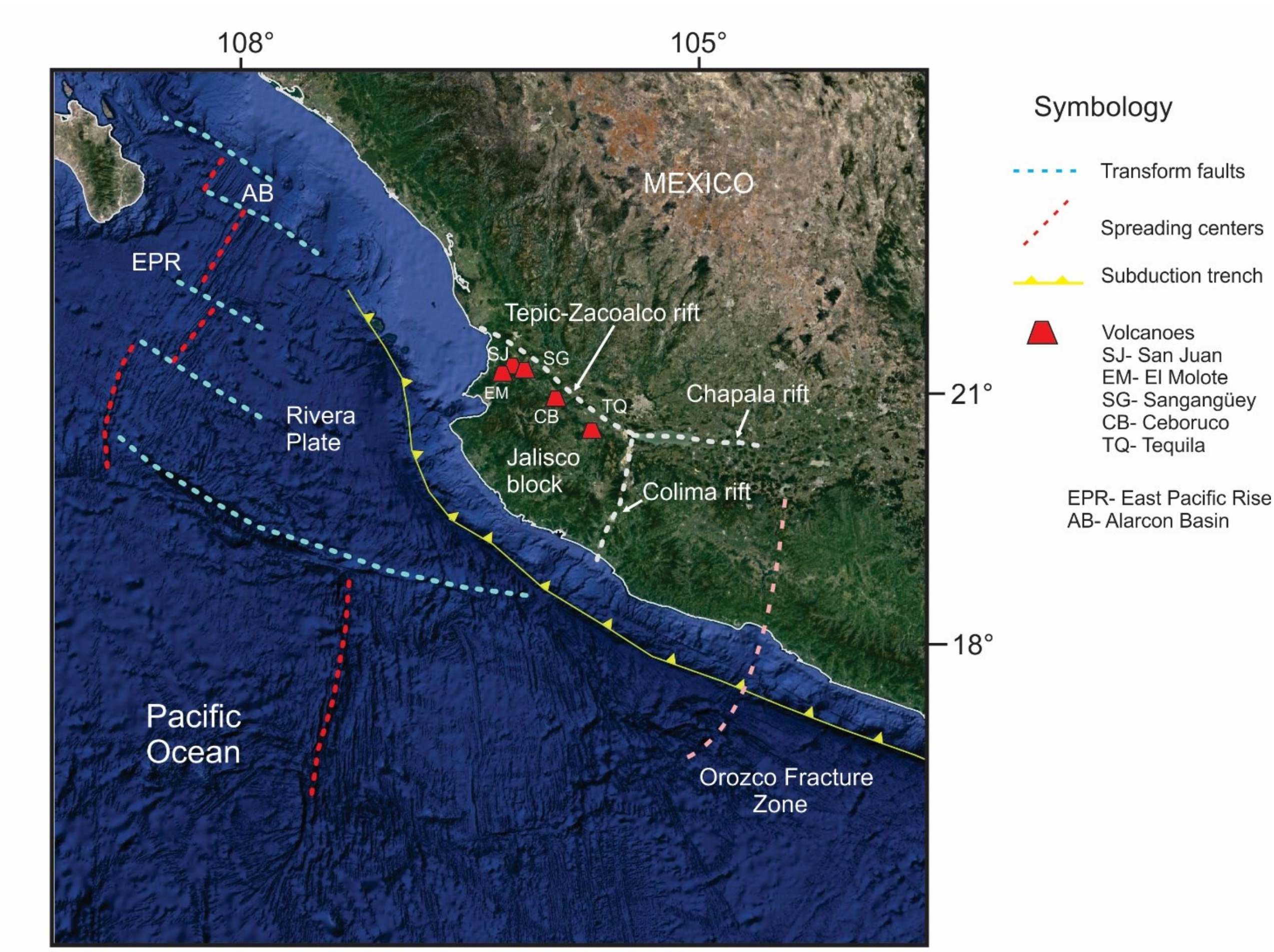

Figure 2: Regional tectonic framework with main elements that interact in the formation of a triple continental junction, volcanoes surrounding the study area: SJ-San Juan Volcano, EM-El Molote Volcano, SG-Sangangüey Volcano, CB-Ceboruco Volcano, TQ-Tequila Volcano (Modified from Stock et al., 1993).

2. METHODOLOGY

For the geochemical exploration of the Mesillas area, Nayarit, three field campaigns were carried out in June, September and November 2018.

2.1 Geological Survey

Geological survey included description in detail and mapping of lithology, structural data and hydrothermal alteration. After field recollection all data were integrated in a Geographic Information System (QGIS®). Additionally, qualitative analyses of fault structural data (orientation, dimension, spatial distributions, fault type and spacing) was done in all observed outcrops.

2.2 Water sampling and chemical analysis

Water samples for chemical analysis were collected in cleaned 250 ml bottles of Nalgene®. The samples collected for the determination of cations were acidified after collection by adding HNO_3 Suprapure® to reach a pH lower than 2. The pH (± 0.1 units), the electrical conductivity (± 0.1 mS / cm) and the temperature (± 0.1 ° C) were measured at the field site using a Thermo Scientific ORION® A329 model portable instrument that was calibrated in the field before sampling. Major cations and anions in water samples were analyzed at the LIG-UNAM (*Laboratorio de Investigación Geoquímica del Instituto de Geofísica de la Universidad Nacional Autónoma de México*). Analyses of the major cations were performed by ionic chromatography with an ICS-900 Thermo Scientific Dionex™ Ion Chromatograph using analytical and quality assurance procedures for geothermal water chemistry following Pang and Armannsson (2006). A Dionex analytical column (250 mm x 4 mm ID) and 20 mM methanesulfonic acid were used as eluent. The ion chromatograph was calibrated with working cation standards. Peaks and retention times were identified with ChromeleonTM software. For the analysis of the main anions, a Metrohm ProfIC-881TM chromatograph with Metrosep ASupp-7 analytical column, an MSM-853-MCO suppressor and a 3.6 mM Na_2CO_3 solution was used as eluent. Peaks and retention times were identified with MagicNetTM software.

Additional samples of untreated water were taken for analysis of stable anions and isotopes (δ^2H and $\delta^{18}O$). Stable isotope analysis of water was conducted at the LIE-UNAM (*Laboratorio de Isótopos Estables del Instituto de Geología de la Universidad Nacional Autónoma de México*). A Model 908-0008-3001 laser absorption spectrometer from Los Gatos Research was used for the ^2H analysis, while a Thermo MAT 253 mass spectrometer with a Thermo Finnigan GASBENCH II couple interface was used for the analysis of ^{18}O. The isotope ratios were converted to per mil delta values using the Vienna Standard Mean Ocean Water (VSMOW; Coplen et al, 1983).

For the analysis of aqueous SiO_2, a Portable Photometer Hach DR-2800 (Hach, 1997) was used. After the samples were collected, CO_3^{-2} and HCO_3^- were measured at the site by titration with 0.02 N HCl using phenolphthalein and methyl orange as indicators with a relative standard deviation of less than 1.5%.

2.3 Diffuse Emission Measurements

Diffuse emissions were measured in the soil and on the surface of the thermal springs. CO_2 flux survey was carried out following the accumulation chamber method using a West Systems instrument (Chiodini et al., 1998) and water surface measurements using a floating chamber (Bernard and Mazot., 2004).

The instrument used is implemented with three detectors for flow measurements: (1) LICOR LI-800, a non-dispersive infrared CO2 sensor with a detection range of 0.1 to 20,000 ppm / s with an accuracy <3% and reproducibility less than 10 % in the range of 0.2 to 10 000 g m^{-2} d^{-1} (2) CH4-WS infrared with flow detection range from 0.02 to 1,444 g m^{-2} d^{-1}, 5% accuracy, 2% repeatability, 22 ppm resolution and ± 25% accuracy in the range of 0.1 - 5 moles m^{-2} d^{-1} and ± 10% in the range of 5 - 150 moles m^{-2} d^{-1} and (3) chemical detector WEST H2S-BH with flow detection range from 0.0002 to 0.6 moles m^{-2} d^{-1}, 3% accuracy. Maximum limit to which the sensor can be subjected (reported by the manufacturer) is 20 ppm (West Systems, 2012).

Diffuse emission fluxes were processed with Wingslib® software (Deutsh, 1998) and Flux Revision of the West System. The methods of graphic statistical analysis (GSA) and sequential Gaussian simulation (sG) were used (Sichel, 1966; Sinclair, 1974; Chiodini et al., 1998; Deutsh, 1998; Cardellini et al., 2003).

3. RESULTS

3.1 Geological mapping

In the study area, there are andesitic lava flows from El Molote volcano. Five andesitic units were identified in an area of approximately 1.5 km^2 where the 25 thermal springs with a temperature between 47-90°C are hosted (Figure 3). The three main discharges have a flow of ~ 27.7, 20.6 and 14.9 liters per second.

The andesitic units have high permeability due to intense fracturing derived from normal fault systems with NW-SE, SW-NE, N-S and E-W trend. (Figure 2). The springs are located mainly in the crossing of NW-SE, SW-NE normal faults and a minor proportion of them in the N-S, E-W faults.

The hydrothermal alteration in the area is of argillic type (Figure 3), with the following mineral association identified with the shortwave infrared spectrometry (SWIR) technique: montmorillonite, illite, opal, calcite, heulandite and goethite. The deposits of these minerals are found in the rocks surrounding the springs in the form of white and reddish crusts where iron oxides occur.

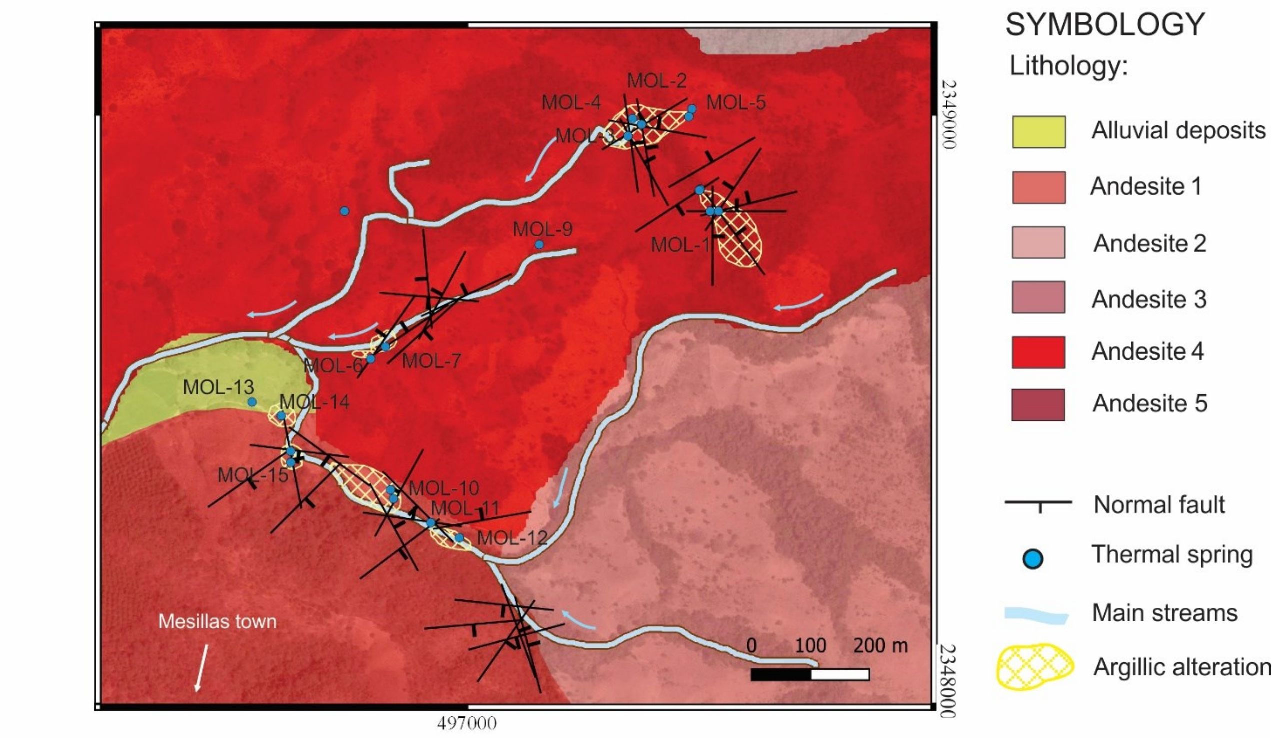

Figure 3: Local geological map with location of thermal springs and major faults that control the location of surface manifestations and location of argillic alteration zones.

3.2 Water chemistry

Electrical conductivity and pH parameters were measured on field (Figure 4a), some samples seem to be diluted with lower electrical conductivity and lower pH. The thermal spring waters are mainly alkaline bicarbonate type (pH between 7.7 to 9.1.) with sodium as major cation (Figure 4b) and the pH and electrical conductivity does not affect the chemical classification of the thermal water.

These thermal waters scattered around the meteoric line indicate meteoric water origin without influence of evaporation but the recharge is not isotopically similar to local meteoric water and probably originates from higher elevation (Figure 5). In the same plot, data (Nayarit, México) reported by Wassenar et al (2009) were included that correspond to local meteoric water.

The Giggenbach diagram (1988) indicates that 65% of the samples are in partial equilibrium; therefore, it is possible to estimate reliable temperatures with cation geothermometers for M2, M7 and M9 samples (Figure 6). It was used the Na/K geothermometer proposed by Fournier (1977) and obtained 117°C, 123°C and 116 °C respectively. Low enthalpy geothermal systems, where reservoir temperatures are between 100 and 150 °C, is kind of controversial. The problem connected with the applicability of geothermometers to low temperature systems concern usually the incorrect understanding of thermodynamics (Nicholson, 1993). Moreover, mixing models and mineral saturation calculations will be evaluated in future studies because cation geothermometers could yield ambiguous results.

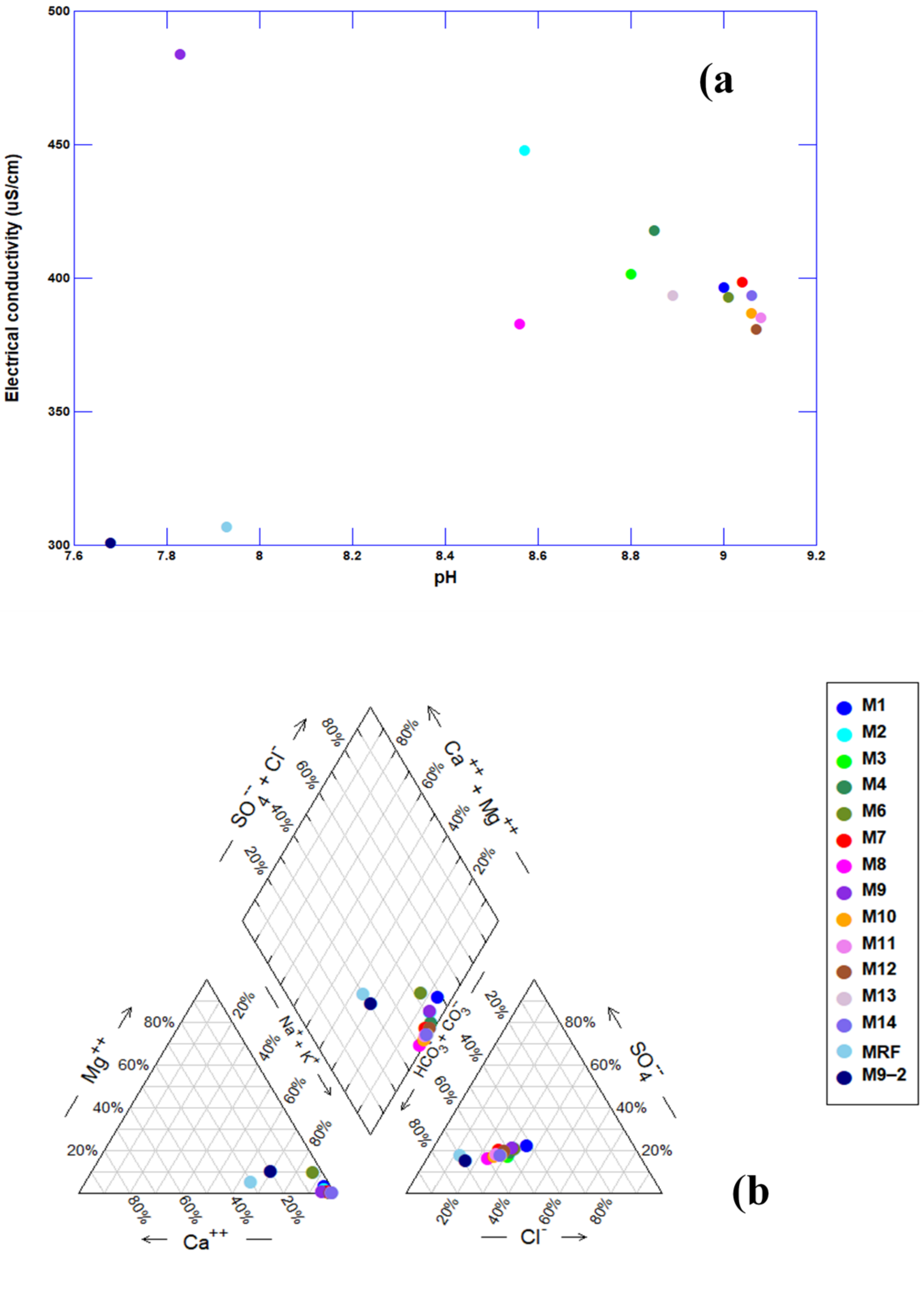

Figure 4: (a) Electrical conductivity, pH and (b) Piper diagram showing water samples from Mesillas geothermal system collected in June and September 2018.

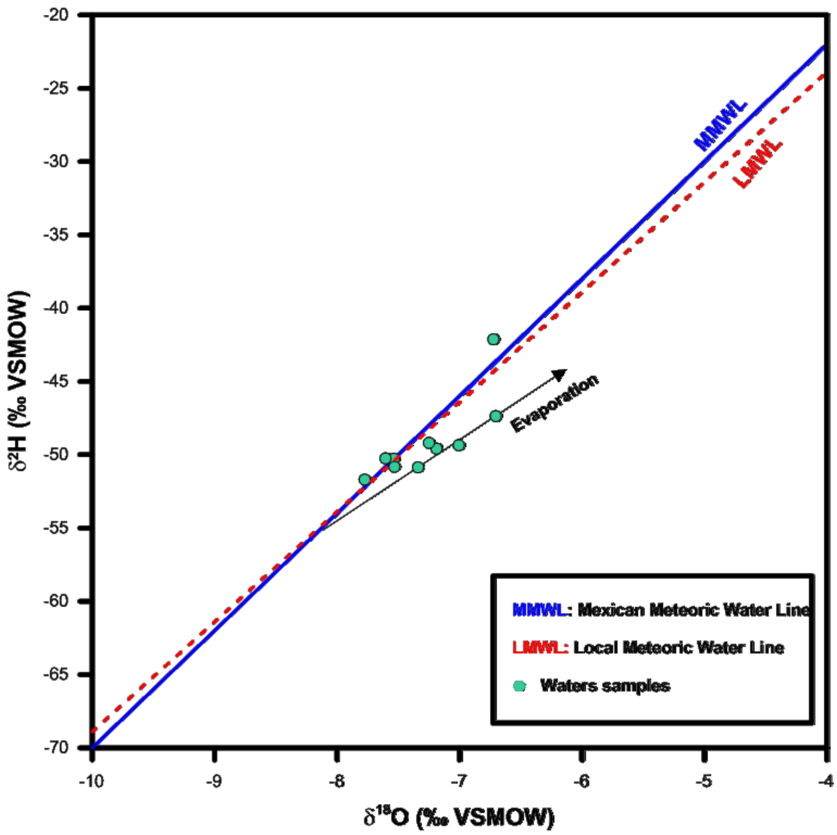

Figure 5: Plot of $\delta^{18}O$ (‰) vs. $\delta^{2}H$ (‰). Thermal water discharged by the hot springs indicates meteoric origin with influence of evaporation process.

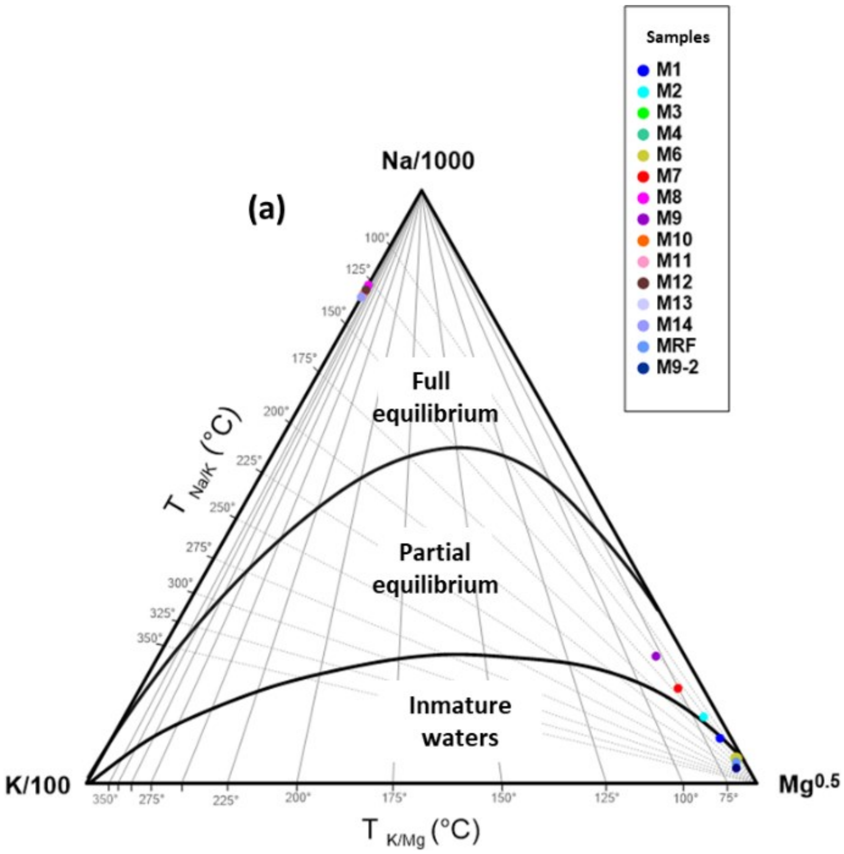

Figure 6: Na-K-Mg equilibrium diagram showing relative concentrations for all the water samples collected in the Mesillas geothermal system. The samples that fall outside of the equilibrium zone are not suitable for geothermometers application. M2, M7 and M9 samples can be used for cation geothermometer.

3.3 Diffuse Emission

During the June - September campaigns 176 points were measured in soils and thermal springs, while in November 30 points were measured in precise locations already detected previously, focused on confirming the anomalous fluxes of CH_4 and H_2S.The main statistical values of all measurements carried out are reported below (Table 1).

Table 1. General results of diffuse emission measurements performed during June and September 2018.

	N total	Mean [g m^{-2} d^{-1}] ± 10%	Standard Deviation	Minimum [g m^{-2} d^{-1}] ± 10%	Maximum [g m^{-2} d^{-1}] ± 10%	Median [g m^{-2} d^{-1}] ± 10%
CO_2	176	45	140	0	1735	18
CH_4	6	185	168	27	494	126
H_2S	102	0.7	1.6	0	9	0.15

Regarding CO_2 fluxes in all area, two groups of degassing were identified with GSA method. An ordinary soil respiration group (A) represented with 60% of the total degassing and a group of hydrothermal origin (B) represented with 40% of the total degassing. This separation in two groups indicates there is an anomalous source of CO_2 degassing in the area confirmed during all field works, mainly in the main thermal springs, and that there is presence of CO_2 degassing in all area. For the contrary, the few locations where H_2S and CH_4 fluxes that were obtained do not allow to do a statistical or spatial analysis. Highest degassing of H_2S was found in thermal springs M13 and M14. The greatest degassing of H_2S was found in the M13 and M14 hot springs. The measured flows exceeded the concentration values allowed in the measuring equipment. No distribution map could be made due to the degassing of H_2S gas is punctual on those springs. There were not high CH_4 flux values in the fieldwork made in September to confirm high values obtained before (June); this can be explained may as an organic source of degassing.

The distribution of the CO_2 fluxes obtained by Gaussian simulation indicates a predominantly punctual degassing on the thermal springs. To perform Gaussian simulation and distribution maps, the outliers were removed (1735 g m^{-2} d^{-1} of CO_2 flux in M2 thermal spring). After the entire process, and according to distribution maps: M3, M6, M8 thermal springs have greater degassing (Figure 5).

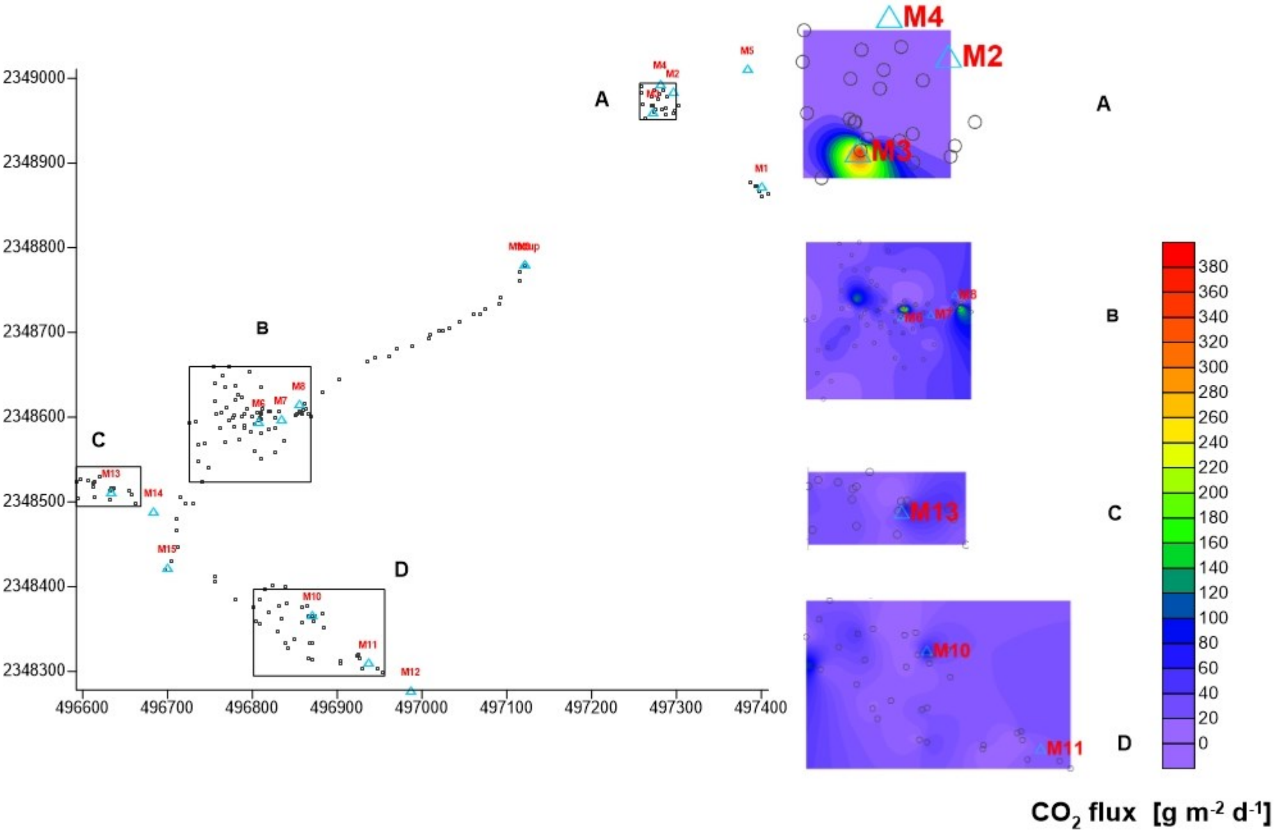

Figure 7: (b) Distribution maps of CO_2 soil flux in Mesillas area. Black empty circles indicate location of main measurement of CO_2 flux made during June and November 2018. Red labels are the names of water samples in each thermal spring. Color scale units are [g m^{-2} d^{-1}] for all maps.

4. FINAL COMMENTS

- A first geochemical and geological exploration was carried out in the Mesillas area, with the discovery of 14 thermal springs (M1-M14) with a temperature range between 47 – 90 ° C and pH range between 7.7 – 9.1.
- Thermal spring waters are mainly basic Na-bicarbonate type.
- These waters have meteoric origin with some samples influenced by an evaporation process. The Na / K geothermometer application is only feasible in three water samples. Temperatures of ~ 117° C, 123° C and 116° C were obtained
- Measurements with significant values are presented in the distribution maps. Values away from the thermal springs were measured, but low values were constantly measured without provide new information to the study area. CO^2 degassing occurs, mainly, in the vicinity of the thermal springs, a preferential direction of degassing is not observed. There is no significant presence of CO^2 degassing in surrounding soils.
- These preliminary results suggest that Mesillas is a low-to-moderate temperature geothermal system. These results will be applied in further studies for investigating the geochemical processes and mixing processes related to the thermal springs in the Mesillas geothermal system.

ACKNOWLEDGMENTS

We want to thank Dr. María de Jesús González-Guadarrama for her technical support in the laboratory. This work was supported by Fondo de Sustentabilidad Energética SENER-CONACyT Grant 207032 of the Centro Mexicano de Innovación en Energía Geotérmica (CeMIE-Geo) project P-01 to R.M. Prol-Ledesma: "Mapas de Gradiente Geotérmico y Flujo de Calor para la República Mexicana".

REFERENCES

Arango-Galván C., Prol-Ledesma R.M., and Torres-Vera, M. A.: Geothermal prospects in Baja California Peninsula. Geothermics, 55, (2015), 39-57.

Bernard, A. and Mazot, A.: Geochemical evolution of the young crater lake of Kelud volcano in Indonesia, In: Wanty, Seal II, (Eds.), 11th Water-Rock interaction Congress, Balkema Publishers, (2004), 4 p.p.

Cardellini, C., Chiodini, G., and Frondini, F.: Application of stochastic simulation to CO2 flux from soil: Mapping and quantification of gas release. J. Geophys. Res. 108, (2003), 2425. DOI:10.1029/2002JB002165

Castillo, H. and De la Cruz, M.: Reconocimiento estructural y volcanológico en la zona termal Domo San Pedro Lagunillas, Nayarit, México, Geofísica Internacional, 31, (1992), 407-415.

Chiodini, G., Cioni, R., Guidi, M., Raco, B., and Marini, L.: Soil CO2 flux measurements in volcanic and geothermal areas. Appl. Geochem. 13, (1998), 543-552. DOI: 10.1016/S0883-2927(97)00076-0

Coplen, T., Brand, W.A., Gehre, M., Gröning, M., Meijer-Harro A.J., Toman, B., and Erkouteren, R. M.: New guidelines for δ13C measurements. Anal. Chem. 78, (2006), 2439–2441.

Craig, S.: The Geochemistry of stable carbon isotopes, Geochimica Cosmochimica Acta, 3, (1953), 53-92.

Deutsch, C.V., Journel, A.G., GSLIB: Geostatistical Software Library and Users Guide, 2nd ed. Oxford University Press, New York, (1998).

Ferrari, L. and Rosas-Elguera, J.: Late Miocene to Quaternary extension at the northern boundary of the Jalisco block, western Mexico: The Tepic-Zacoalco rift, Tectonics and Volcanism of Mexico, Geol. Soc. of Am., Special Paper, 334, (2000), 42-64.

Ferrari, L., Petrone, C., Francalanci, L., Tagami, T., Eguchi, M., Conticelli, S., Manetti, P., and Venegas-Salgado, S.: Geology of the San Pedro-Ceboruco graben, western Trans-Mexican Volcanic Belt: Revista Mexicana de Ciencias Geológicas, 20, (2003), 165-181.

Ferrari, L., Tagami, T., Eguchi, M., Orozco-Esquivel, M. T., Petrone, C., Jacobo-Albarrán, J., and López-Martínez, M.: Geology, geochronology and tectonic setting of late Cenozoic volcanism along the southwestern Gulf of Mexico: the Eastern Alkaline Province revisited: Journal of Volcanology and Geothermal Research, 146, (2005), 284-306.

Fournier, R.O.: Chemical geothermometers and mixing models for geothermal systems, Geothermics, 5, (1977), 41-50.

Giggenbach, W.: Geothermal solute equilibria. derivation of Na-K-Mg-Ca geoindicators. Geochimica et Cosmochimica Acta, 52, (1988), 2749-2765.

Gómez-Tuena, A., Orozco-Esquivel, M.T., and Ferrari, L.: Igneous petrogenesis of the Transmexican Volcanic Belt. In: Alaniz-Álvarez, S.A., Nieto-Samaniego, A.F. (Eds.), Geology of México: Celebrating the Centenary of the Geological Society of México. Geological Society of America Special Paper Vol. 422, (2007), 129–181.

Hach: Portable laboratory manual. Loveland, CO, USA, (1997).

Iglesias, E.R., Torres, R.J., Martinez-Estrella, J.I., and Reyes-Picasso, N.: Summary of the 2014 Assessment of Medium- to Low-Temperature Mexican Geothermal Resources, Proceedings World Geothermal Congress 2015, Melbourne, Australia. (2015), Paper 16081, 7pp.

Nicholson, K.: Geothermal Fluids: Chemistry and Exploration Techniques, Springer-Verlag, Berlin Heidelberg, (1993).

Pang, Z., Ármannsson, H.: Analytical Procedures and Quality Assurance for Geothermal Water Chemistry 1 UNU-GTP, Iceland Report, (2006), 172 pp.

Romo-Jones, J.M., Gutiérrez-Negrín, L.C.A., Flores-Armenta, M., del Valle, J.L., and García, A.: 2016 Mexico Country Report IEA Geothermal. (2017), 10 pp.

Righter, K., Carmichael, I., Becker, T., and Renne, R.: Pliocene to Quaternary volcanism and tectonics at the intersection of the Mexican Volcanic Belt and the Gulf of California: Geological Society of America Bulletin, 107, (1995), 612-626.

Schaaf, P., Morán-Zenteno, D., Hernández-Bernal, M., Solís-Pichardo, G., Tolson, G., and Köhler, H.: Paleogene continental margin truncation in southwestern Mexico: geochronological evidence: Tectonics, 14(5), (1995),1339-1350.

Sinclair, A.J.: Selection of threshold values in geochemical data using probability graphs. J. Geochem. Explor. 3, (1974), 129-149.

Stock, J. M.: Tectónica de placas y la evolución del Bloque de Jalisco, México, GEOS, Bol. UGM, 13, (1993), 3-9.

Urrutia-Fucugauchi, J., and Rosas-Elguera, J.: Paleomagnetic study of the eastern sector of Chapala lake and implications for the tectonics of west-central Mexico, Tectonophysics, 239, (1994), 61-71.

Wassenaar, L.I., Van Wilganburg, S.L., Larson, K., and Hobson, K.A.: A groundwater isoscape (D, 18O) for Mexico. Journal of Geochemical Exploration, 102, (2009), 123–136.

West Systems. Portable diffuse flux meter with LI-COR CO2 detector, Handbook, West Systems srl, Italy, (2012)